Lipid peroxidation is involved in calcium dependent upregulation of mitochondrial metabolism in skeletal muscle

Afnan Saleh Al-Menhali[1,2], Sameem Banu[1], Plamena R. Angelova[3,5], Andrei Barcaru[4], Peter Horvatovich[4], Andrey Y. Abramov[3,*], Morana Jaganjac[1,2,*,#]

[1]Qatar Analytics & BioResearch Lab, Anti Doping Lab Qatar, Doha, Qatar
[2]Division of Medicine, UCL, London, UK
[3]Department of Clinical and Movement Neuroscience, UCL Institute of Neurology, London, WC1N 3BG, UK
[4]Groningen Research Institute of Pharmacy, University of Groningen, Groningen, 9713 AV, Netherlands
[5]Department of Pathophysiology, Sechenov First Moscow State Medical University, 119048 Moscow, Russia

Running title: Lipid peroxidation mediates myotube mitochondrial metabolism

* Correspondence should be addressed to Andrey Y. Abramov (email: a.abramov@ucl.ac.uk) or to Morana Jaganjac (email: m.jaganjac@ucl.ac.uk)
# Lead Contact: M.J. (email: m.jaganjac@ucl.ac.uk)

Abbreviations:

2',7'-dichlorfluorescein-diacetate (DCFH-DA); 4-hydroxynonenal (4-HNE); adenosine triphosphate (ATP); carbonyl cyanide p-(trifluoromethoxy)phenylhydrazone (FCCP); cytosolic calcium concentration ($[Ca^{2+}]_c$); dihydroethidium probe (DHE); Dulbecco's Modified Eagle's Medium (DMEM); extracellular acidification rates (ECAR); fetal bovine serum (FBS); gene of interest (GOI); horse serum (HS); housekeeping gene (HKG); lipid peroxidation (LPO); oxygen consumption rates (OCR); polyunsaturated fatty acids (PUFA); reactive oxygen species (ROS); relative fluorescence units (RFU); threshold cycle (C_T)

Summary

Background: Skeletal muscle cells continuously generate reactive oxygen species (ROS). Excessive ROS can affect lipids resulting in lipid peroxidation (LPO). Here we investigated the effects of myotube contraction on the LPO induction and the impact of LPO-product 4-hydroxynonenal (4-HNE) on physiology/pathology of myotubes using C2C12 myoblasts.

Methods: C2C12 myoblasts were differentiated into myotubes, stimulated with caffeine and analyzed for the induction of LPO and formation of 4-HNE protein adducts. Further effects of 4-HNE on mitochondrial bioenergetics, NADH level, mitochondrial density and expression of mitochondrial metabolism genes were determined.

Results: Short and long-term caffeine stimulation of myotubes promoted superoxide production, LPO and formation of 4-HNE protein adducts. Furthermore, low 4-HNE concentrations had no effect on myotube viability and cellular redox homeostasis, while concentrations from 10μM and above reduced myotube viability and significantly disrupted homeostasis. A time and dose-dependent 4-HNE effect on superoxide production and mitochondrial NADH-autofluorescence was observed. Finally, 4-HNE had strong impact on maximal respiration, spare respiratory capacity, ATP production, coupling efficiency of mitochondria and mitochondrial density.

Conclusion: Data presented in this work make evident for the first time that pathological 4-HNE levels elicit damaging effects on skeletal muscle cells while acute exposure to physiological 4-HNE induces transient adaptation.

General significance: This work suggests an important role of 4-HNE on the regulation of myotube's mitochondrial metabolism and cellular energy production. It further signifies the importance of skeletal muscle cells hormesis in response to acute stress in order to maintain essential biological functions.

Keywords

4-hydroxynonenal; lipid peroxidation; reactive oxygen species; calcium oscillations; NADH; mitochondrial metabolism

Introduction

Our movement is controlled by skeletal muscles. Intensity of our daily movements, including exercise, activates multiple processes in our muscle's cells for maintenance of energy metabolism and cell signaling. Contraction of the skeletal myocytes is controlled by calcium. Each peak of calcium rise is corresponding to contraction and activation of the frequency of calcium oscillations that lead to increased frequency of muscle contractions. Considering this, the number of studies used different calcium stimulus to induce calcium oscillations in muscle cells for induction of contraction and mimicking exercise in cell cultures (Ding et al., 2012).

The many roles of mitochondria in cell physiology and their involvement in signaling pathways have received much attention recently. However, their major role remains the canonical role of generating adenosine triphosphate (ATP), the main energy currency of the organism, by converting energy from the oxidation of macronutrients. Central to the maintenance of energy homeostasis in normal physiology is the ability to match energy production to meet changes in energy demand. This is especially true in skeletal muscle, where energy demands change with levels of activity, and where a failure to adapt energy supply appropriately will lead to a failure of adequate muscle function. Indeed, it seems likely that such failures underlie changes in muscle physiology associated with ageing, immobilization and a variety of disease states (Huang and Hood, 2009; Kim et al., 2008). In the short term, changes in bioenergetic efficiency may be largely mediated by the transfer of calcium signals integral to the process of EC coupling to the mitochondria, where several mechanisms together serve to increase the efficiency of oxidative phosphorylation (Duchen, 1999).

Skeletal muscle possesses an amazing plasticity in response to physical stress such as exercise (Steinbacher and Eckl, 2015). Contracting skeletal muscle cells are marked with a variety of phenotypic and physiological responses, including increased release of endogenous calcium and production of reactive oxygen species (ROS) and upregulation of 5′-adenosine monophosphate-activated protein kinase (AMPK). Rapid changes of cytosolic calcium levels is required for contraction and relaxation of skeletal muscle and can contribute to cellular protein turnover as well as to removal of affected organelles (Grumati and Bonaldo, 2012). AMPK is one of key players in the skeletal muscle metabolism as it serves as an indicator of cellular energy status (Lantier et al., 2014). ROS are normally produced in resting muscle cells, but their formation is

increased with muscle contraction. Among ROS produced by the skeletal muscle is superoxide anion that is generated endogenously in the inner membrane of mitochondria during the respiration or by the action of NADPH oxidase associated with sarcoplasmic reticulum (Pattwell et al., 2004), transverse tubules (Hidalgo et al., 2006), plasma membrane NADPH oxidase (McArdle et al., 2001) and phospholipase A2-dependent process (Gong et al., 2006). Moderate ROS formation has a beneficial effect and plays one of the key roles in skeletal muscle adaptation to exercise (Gomez-Cabrera et al., 2008). Contrary, excessive ROS production is toxic and can cause oxidative damage to macromolecules and promote oxidative stress (Esterbauer et al., 1991). Peroxidation of lipids (LPO) is considered to be one of the most important mechanisms of cell injury under condition of oxidative stress and is shown to be involved in the pathology of numerous diseases. Polyunsaturated fatty acids (PUFAs) are susceptible to ROS induced damage yielding reactive aldehydes, such as 4-hydroxyalkenals and other similar α, β-unsaturated aldehydes (Uchida, 2003). LPO-derived aldehydes, among which is 4-hydroxynonenal (4-HNE), are more stable than ROS and can therefore diffuse across membranes and reach the targets distant from the initial site of oxidative injury (Zarkovic, 2003; Jaganjac et al., 2013) altering signaling pathways either directly or through functional modification of macromolecules (Leonarduzzi et al., 2004; Biasi et al., 2006; Jaganjac et al., 2010). 4-HNE was shown to play a role in mitochondrial ROS production (Parker, et al., 2008). Importantly, lipid peroxidation is essential for phospholipase activity, including phospholipase C, which produced IP3-dependent calcium signal and modify cell signaling (Vaarmann et al., 2010; Domijan et al., 2014; Angelova and Abramov, 2016).

Mitochondrial activity and function in skeletal muscle is a highly controlled process, under the influence of a variety of nuclear and mitochondrial factors that act as metabolic sensors and can adapt to perturbations in cellular nutrient and energy status. Increase of the energy demand in the time of physical exercises in skeletal muscles leads activation of ATP production.

The effect of exercise induced oxidative stress on the LPO of muscle cells and its later impact on mitochondrial performance remains to be elucidated. Additionally, the effect of 4-HNE on mitochondrial metabolism has not been tested, although 4-HNE has been shown to modify mitochondrial proteins (Andringa et al., 2014; Zhao et al., 2014). Thus, in the present study we were aiming to test if prolonged calcium signaling and

contractions in muscle cells activates lipid peroxidation and how product of lipid peroxidation regulates physiological and pathological processes in mitochondria.

Materials and Methods

Cell culture and myoblast differentiation

Mouse myoblast C2C12 cell line was obtained from ATCC (ATCC Number CRL-1772, USA). The cells were grown as monolayer in Dulbecco's Modified Eagle's Medium (DMEM) supplemented with 10% fetal bovine serum (FBS, Sigma, Germany) and 1% Penicillin/Streptomycin (Sigma, Germany) at 37°C in a humidified atmosphere containing 5% CO_2.

Cells were seeded on a 22mm round coverslips for imaging experiments, in Seahorse cell culture 24-well plate at a density 8 x 10^3 for the measurement of mitochondrial metabolism or in 96-well plates at a density 6 x 10^3 cells per well for all other assays.

When cells reached 70% to 80% confluence, media was replaced with DMEM supplemented with 2% horse serum (HS, Sigma, Germany) to induce myoblasts differentiation into myotubes. The differentiation of myoblasts was evaluated daily using Olympus IX53 inverted light microscope. All experiments were performed on myotubes that were 5-8 of differentiation days.

4-HNE preparation

The aldehyde was obtained in the form of 4-Hydroxynonenal-dimethylacetal (Enzo Life Science) and prepared similarly as described before (Zivkovic et al., 2005). Prior to the experiment it was activated with 1 mM cold HCl for 1 hour at 4°C. For the experiment HNE was diluted in DMEM medium.

Viability assay

Myotubes were treated with ranging concentrations of caffeine (1 mM, 5 mM and 10 mM) for 2 hours or left untreated as control.

Myotubes were treated in low serum media (2% HS) with ranging concentrations of 4-HNE (5 μM, 10 μM, 25 μM, 50 μM, 75 μM and 100 μM) overnight or left untreated to serve as a control. The AlamarBlue assay was used to assess the impact of caffeine and 4-HNE on the viability of the cells (Ex 570 nm / Em 600 nm).

Measurement of cytosolic calcium $[Ca^{2+}]_c$

Cytosolic calcium concentration $[Ca^{2+}]_c$ was monitored in single cells using Fura-2 as previously described (Domijan and Abramov, 2011). Briefly, myotubes were loaded with 5 μM Fura-2 AM (Molecular Probes) for 30 minutes at room temperature in the presence of 2% Pluronic acid in HBSS buffer. Cells were illuminated with Xenon arc lamp (excitation 340 and 380 nm) and emission above 500 nm was recorded using cooled CCD camera. $[Ca^{2+}]_c$ transients are shown as ratio of excitations (340/380 nm).

Kinetic measurement of changes in cellular redox homeostasis

The impact of caffeine and 4-HNE on ROS generation was measured using dihydroethidium probe (DHE, Molecular Probes). The fluorescence was continuously measured every 15 seconds for 40 minutes, and then as a single point after 24h using Tecan M200 Pro reader (Ex 530 nm / Em 580 nm).

Additionally, the impact of 4-HNE and caffeine on intracellular ROS production was measured using 2',7'-dichlorfluorescein-diacetate (DCFH-DA, Fluka) assay as previously described (Poljak-Blazi et al., 2011; Elrayess et al., 2017). Cells were loaded with 10 μM DCFH-DA for 30 minutes at 37°C. The excess probe has been removed, treatment added, and fluorescence intensity continuously measured throughout 8 hours at 37°C and 5% CO_2 using TECAN Infinite M200 PRO plate reader equipped with gas control mode, excitation wavelength at 500 nm and emission at 529 nm. The arbitrary units, relative fluorescence units (RFU), were based directly on fluorescence intensity.

Measurement of lipid peroxidation with C11-BODIPY (581/591) assay

The ability of caffeine to induce lipid peroxidation was investigated using lipid peroxidation sensor C11-BODIPY (581/591) (1 μM; Molecular Probes, USA). C11-BODIPY581/591 is a lipophilic ratiometric fluorescent dye for indexing lipid peroxidation in cellular membranes.

Myotubes were treated with caffeine (0, 1, 5 and 10 mM) for 2 hours for two consecutive days. After 24 and 48 h of treatment myotubes were loaded with 1 μM C11-BODIPY (581/591) for 30 min at 37°C. The rates of lipid peroxidation were measured using TECAN M200 Pro Multimode reader with excitation/emission of 495/521 nm for the green signal (oxidized) and 575/600 nm for the red signal (non-oxidized). Images were recorded with the ArrayScan XTI (Thermo) using 485-20 nm filter and 25 fields per well were imaged. Lipid peroxidation is presented as ratio of oxidized: non-oxidized C11-BODIPY (581/591).

NADH autofluorescence assay

NADH and its oxidized form NAD+ act as hydrogen carriers at the site of the electron transport chain during mitochondrial respiration. The fluorescent properties of NADH make it a valuable fluorescent indicator of the mitochondrial metabolic state. The impact of 4-HNE on mitochondrial level was performed according to the protocol described before (Bartolome et al., 2017). NADH autofluorescence was excited at 351 nm (using Xennon arc lamp and monochromator) and measured at 375-470 nm was recorded using cooled CCD camera.

Measurement of oxygen consumption with XFe24 flux analyzer

The immediate effect of 4-HNE and the effect of 24 hours upon treatment on the oxygen consumption in C2C12 myotubes was determined using XFe Cell Mito Stress Test kit (Seahorse Bioscience Inc., USA). To assess the immediate effect the myotubes were serum starved for 1 hour in Seahorse XF Base Medium supplemented with 2 mM glutamine, 1 mM pyruvate and 10 mM glucose at 37ºC in a humidified atmosphere without CO_2. Modified protocol utilizing 4 ports has been used with 4-HNE (0, 2.5, 5 and 10 µM final) being set as a first injection (port A) while oligomycin (1 µM final), mitochondrial uncoupler carbonyl cyanide p-(trifluoromethoxy)phenylhydrazone (FCCP, 0.5 µM final) and rotenone/antimycin A (0.5 µM final) were loaded onto ports B, C and D, respectively. Three basal oxygen consumption rate (OCR) measurements were performed using the Seahorse XFe24 Extracellular Flux Analyzer (Seahorse Bioscience Inc., USA), myotubes stimulates with 4-HNE for 60 min followed by the injection of oligomycin, FCCP, and rotenone/antimycin A. Extracellular acidification rates (ECAR, mpH/min) and OCR (pmol/min) are measured three times in 5-replicate wells except for 4-HNE treatment when measured 8 times.

For long term effect of 4-HNE exposure, 24 hours upon treatment cells were serum starved as described above and ECAR and OCR assessed XFe cell mito stress test kit according to manufacturer's instructions.

The Seahorse XFe Cell Mito Stress Test Report Generator was used to automatically calculate assay parameters as absolute OCR in pmol O_2/min. Maximal Respiration is calculated as a difference between maximum OCR measurement after FCCP injection and minimum OCR measurement after rotenone/antimycin A injection. ATP production is calculated as a difference between last OCR measurement before

Oligomycin injection and minimum OCR measurement after Oligomycin injection. Finally, Spare Respiratory Capacity is calculated as a difference between Maximal and basal respiration.

Measurement of caffeine-induced formation of 4-HNE protein adducts formation

Myoblasts were seeded in 24-well plates with density of 2×10^5 , differentiated into myotubes and treated with caffeine (0, 1 mM, 5 mM and 10 mM) for 2 hours for three consecutive days. Then, proteins were isolated from myotubes and their concentration were measured using BCA Protein Assay Kit (Pierce). The effect of caffeine on the production of 4-HNE protein adducts was measured using HNE Adduct Competitive ELISA kit (Cell Biolabs).

RNA extraction and real-time PCR

Myotubes were treated overnight with 4-HNE (2.5 µM, 5 µM and 10 µM) or left untreated as a control. Total RNA was isolated using RNeasy Mini Kit (Qiagen). Followed by measuring RNA quantity using NanoDrop 2000 spectrophotometer (Thermo Scientific). For the reverse transcription of cDNA, RT² First Strand Kit (Qiagen) was used. Then, real-time PCR was performed using Mouse Mitochondrial Energy Metabolism (PAMM-008Z) RT^2 Profiler PCR Arrays (Qiagen). The PCR arrays provide analysis of 84 genes involved in the expression of mitochondrial respiration and biogenesis.

Measurement of mitochondrial density

Myotubes were treated with 4-HNE overnight. Stained with 200 nM MitoTracker Green FM (Molecular Probes) for 45 min and 2 µg/mL Hoechst (33342, Molecular Probes) for 10 min at 37°C. Fluorescence intensity of MitoTracker was measured using TECAN Infinite M200 PRO plate reader (Ex 490 nm/ Em 516 nm). Myotubes were imaged using ArrayScan XTI (Thermo) with 386-23 nm filter for Hoechst and 485-20 nm filter for MitoTracker.

Statistics

All experiments were repeated at least 3 times. Descriptive statistics were shown as the mean ± standard deviation (SD). The significance of differences between groups was assessed using the Student t-test and Chi-square test. When more than two groups were

compared, we used one sided ANOVA with appropriate post hoc testing. The SPSS 16211.01 for Microsoft Windows were used. Differences with P less than .05 were considered statistically significant

Data analysis of PCR array data was preceded by the pre-processing step, i.e. normalization. More specifically the following steps were applied:

1. From the threshold cycle (C_T) values of each gene of interest (GOI), the house keeping gene (HKG) C_T value was subtracted: $\Delta C_T = C_T(GOI) - C_T(HKG)$
2. Average ΔC_T was calculated for each group: $\overline{\Delta C_T} = \frac{\sum_{i=1}^{N} \Delta C_T}{N}$. Here, N is the number of replicates within one group. At this stage, further statistics can be applied with the average ΔC_T of each group.
3. For the expression values, the $\Delta\Delta C_T$ is calculated between each treatment group and control group: $\Delta\Delta C_T = \overline{\Delta C_T}(Group\ i) - \overline{\Delta C_T}(Control)$
4. Fold change is further calculated using the values from step 3: $FC = 2^{-\Delta\Delta C_T}$

Results

Caffeine induces dose-dependent calcium oscillations in myotubes

In order to establish the optimal caffeine concentration to promote prolonged repetitive $[Ca^{2+}]_c$ signals equivalent to prolonged activity, we first examined the $[Ca^{2+}]_c$ signals generated by a range of caffeine concentrations using live cell imaging. As expected, application of caffeine induced dose-dependent $[Ca^{2+}]_c$ changes in myocytes (Figure 1). These were characterised by oscillatory changes in $[Ca^{2+}]_c$ that increased in frequency with increasing caffeine concentrations eventually merging to a high $[Ca^{2+}]_c$ plateau at higher caffeine concentrations (>10mM). Exposure of myocytes to 1mM caffeine induced $[Ca^{2+}]_c$ peak (Figure 1A, n=85 cells). Each $[Ca^{2+}]_c$ transient coincided with a myotube contraction (Figure 1 ?). Stimulation of the cells with 5 mM caffeine induced an initial $[Ca^{2+}]_c$ spike followed by sustained $[Ca^{2+}]_c$ repetitive oscillations that continued as long as we continued to observe them (Figure 1B; n=85 cells), while 10 mM caffeine produced an even larger increase in $[Ca^{2+}]_c$ which reached a plateau after about 1 min (Figure 1C; n=95). Caffeine induce calcium signal via activation of ryanodine receptor and release of Ca^{2+} from sarcoplasmic reticulum and in our experiments, it was confirmed by inhibition of the caffeine-induced calcium signal by specific for ryanodine receptor inhibitor dantrolene (Figure 1D, n=45).

Given these responses, we chose to use 1mM as a mechanism to induce a reasonably 'physiological' level of myotube activity resembling the activity of exercise, 5mM to stimulate a near maximal $[Ca^{2+}]_c$ signal while 10 mM appears to cause potentially damaging $[Ca^{2+}]_c$ overload.

Caffeine-induced calcium signal in myotubes activates superoxide production

It should be noted that the selected caffeine concentrations were not toxic for C2C12 myotubes (Figure 2A, $p>0.05$). The ability of caffeine to induce superoxide production and peroxidation of lipids in myotubes is presented in Figure 2. Kinetic measurement of intracellular ROS production with DHE in myotubes showed time and dose dependent effect of caffeine on this process. The lowest caffeine concentration (1 mM) induced 15 % higher rate of ROS production 30 minutes after addition of treatment ($P>0.05$, Figure 2B and C). The 5- and 10-mM caffeine produced more prominent stimulation of the rate of ROS generation in myotubes by 45 % and 80 % compared to control untreated myotubes ($P<0.05$ for both, Figure 2B and C). Importantly, preincubation of the myotubes with 20 μM dantrolene completely block caffeine (10mM)-induced ROS production (n=56; Figure 1 B, C) that confirm Ca^{2+}-dependence of ROS production.

Caffeine activated ROS production induces lipid peroxidation in myotubes.

Application of 1 mM caffeine had a small or no effect ($P>0.05$) on lipid peroxidation 24 and 48 hours after myotubes exposure to caffeine treatment (Figure 2D and E) while the peroxidation of lipids was strongly increased in myotubes 24 and 48 hours upon treatment with 5 and 10 mM caffeine ($P<0.05$, for both, Figure 2D and E). Further experiment confirmed that caffeine treatment induced dose dependent increase in 4-HNE protein adducts in C2C12 myotubes (Figure 2F),

The impact of lipid peroxidation on myotubes was further assessed using 4-HNE, a very well-studied bioactive product of lipid peroxidation (Figure 3). Both physiologically relevant (2.5 μM and 5 μM) and higher 4-HNE concentrations (≥10 μM) were used.

Product of lipid peroxidation activates non pathological production of ROS

Although caffeine-induced lipid peroxidation is due to increased ROS production, product of lipid peroxidation also could be a trigger for further changes in viability and

redox balance in myotubes. Thus, the physiological level of 4-HNE (5 μM) showed no effect on myotubes viability ($P>0.05$) while higher supraphysiological 10 μM 4-HNE concentration decreased viability by 20%. Pathological concentrations tested, >10 μM to 100 μM decreased viability from 20% down to 75%, respectively ($P<0.05$, Figure 3A and B). Furthermore, 4-HNE was shown to alter cellular redox homeostasis in time and dose dependent manner (Figure 3C and D). Pathological concentrations of 4-HNE (50 μM, 75 μM and 100 μM) promoted production of intracellular ROS, mainly H_2O_2 as measured by DCFH-DA assay ($P<0.05$, Figure 3C). Contrary, treatment of myotubes with lower 4-HNE concentrations did not show a significant increase in intracellular H_2O_2 production ($P>0.05$, Figure 3C). Interestingly, although 10 μM 4-HNE treatment of myotubes did not show significant impact on H_2O_2 production it strongly promoted intracellular superoxide production ($P<0.05$, Figure 3D).

Regulation of mitochondrial metabolism by a byproduct of lipid peroxidation

Based on the results of caffeine induced formation of 4-HNE protein adducts in myotubes and dose response effects of 4-HNE on myotube viability the concentrations 2.5 μM, 5 μM and 10 μM were selected to approximate those of low to moderate levels of physiological oxidative stress for 4-HNE functional studies on mitochondria metabolism.

NADH is a donor of electron for complex I of mitochondrial electron transport chain. Effect of 4-HNE on autofluorescence of NADH was dependent on concentration (Figure 4A). Thus, 2.5 μM 4-HNE induces increase of mitochondrial NADH level that can suggest inhibition of the complex I –related respiration or activation of NADH production (Figure 4A upper right). Application of 5 μM 4-HNE induce mild and 10 μM more strong decrease in NADH level (Figure 4A lower left and right, respectively). Application of 1 μM FCCP at the end of the experiment (which maximally activates respiration with consumption of all mitochondrial NADH) and inhibitor 1 mM NaCN (which block consumption of NADH in mitochondria) confirm increased mitochondrial pool of NADH by 2.5 μM and decrease by 5 and 10 μM of 4-HNE (Figure 4A).

The maximal respiration and spare respiratory capacity were inhibited in myotubes treated with 2.5 μM and 5 μM 4-HNE ($P<0.05$ for all, Figure 4B and C). Interestingly, no effect on the same was seen when myotubes were exposed to 10 μM 4-HNE ($P>0.05$ for all, Figure 4 B). However, all concentrations inhibited ATP production. Twenty-

four hours upon exposure of myotubes to 5 μM 4-HNE the maximal respiration, spare respiratory capacity and ATP production were recovered to control level (Figure 5A and B). Although, 10 μM 4-HNE had no immediate effect, 24 h upon exposure strong inhibition of maximal respiration, spare respiratory capacity and ATP production was observed (Figure 5A and B). Furthermore, 8 hours post treatment, myotubes treated with 10uM 4-HNE showed 40% increase in the superoxide production compared to control (Figure 5C).

The effect of acute 4-HNE exposure revealed 11 mitochondrial metabolism genes up regulated 24 hours upon 4-HNE treatment in a dose dependent manner (Figure 5D and G). The strongest effect was observed for the mitochondrial Complex I (NADH dehydrogenase) by upregulating even 5 genes (Ndufb9, Ndufc1, Ndufs7, Ndufv1 and Ndufv3). 4-HNE also upregulated Sdhc and Sdhd genes of Complex II (Succinate dehydrogenase), Uqcrc1, Uqcrc2 and Uqcrh genes of Complex III (Cytochrome c reductase) and only one gene, Atp6v0d2 belonging to Complex V (ATP synthase). Moreover, an acute 4-HNE exposure triggered and increase in mitochondrial density 24 hours later in a dose dependant manner (Figure 5E and F).

Discussion

In response to exercise and increased ROS production polyunsaturated fatty acids that are esterified in the myotubes' membranes are susceptible to ROS induced damage yielding 4-HNE formation (Jaganjac et al., 2016). Bioactive LPO end product, 4-HNE, in one of the main molecules in stress mediated signaling (Yang et al., 2003) and due to its relative abundance in cells and tissues can exert either physiological or pathological effects (Chapple et al., 2013; Schaur et al., 2015). Under physiological conditions (up to 5 μM) 4-HNE activates signaling cascades, transcription factors and aldolase reductase metabolism while higher 4-HNE concentrations can induce cellular dysfunction, apoptosis and autophagy (Chapple et al., 2013). This study reports for the first time the possible pathophysiological effects of exercise induced 4-HNE on the mitochondria of skeletal muscle cells demonstrating modulatory role of 4-HNE essential for the normal myotube function. To investigate pathophysiological responses of skeletal muscle to low, moderate and intense exercise, based on the caffeine induced oscillatory changes in $[Ca^{2+}]_c$, caffeine concentrations of 1mM, 5mM, and 10 mM respectively, were selected.

Media supplementation with caffeine promoted myotube contraction and altered cellular redox homeostasis by inducing superoxide production in myotubes. Indeed, myotube contraction is known to promote ROS formation that can have beneficial adaptation effect to exercise or in the case of ROS overproduction detrimental effects in skeletal muscle cells (Cheng et al., 2016). Caffeine induced ROS formation, consequently promoted peroxidation of lipids and formation of 4-HNE conjugates in a dose dependent manner. 4-HNE protein modification can alter protein structure and function affecting protein processing, trafficking and normal cellular function (Zarkovic et al., 2013; Jaganjac et al., 2012) but can also trigger further changes in the myotube viability and cellular redox balance. Indeed, our data show that 4-HNE alters cellular redox homeostasis in time and dose dependent manner. Physiological 4-HNE concentrations did not affect cellular viability and did not induce neither intracellular H_2O_2 nor superoxide production within the first few hours of exposure to 4-HNE. Contrary, higher 4-HNE concentrations exerted pathological effects on myotubes, strongly affecting the viability of myotubes and immediately altering cellular redox homeostasis. However, 8 hours after acute exposure to 10 μM 4-HNE, cellular superoxide production was significantly induced but the same was not observed in the case of H_2O_2 production rendering myotubes less susceptible to 4-HNE induced H_2O_2 formation compared to other cells, such are adipocytes (Elrayess et al., 2017).

Although physiological 4-HNE concentrations did not seem to affect the myotube viability and cellular redox homeostasis the immediate effect of all concentrations tested impaired ATP synthesis. Furthermore, the immediate effect of physiological 4-HNE also reduced maximal respiration, spare respiratory capacity and coupling effect suggesting that immediate 4-HNE stress mediates mitochondrial dysfunction in myotubes. An increased ATP demand can cause mitochondrial overburden impairing mitochondrial functions like oxygen consumption and ATP synthesis promoting further ROS production that can trigger an adaptive cellular response or eventually induce autophagy (Filomeni et al., 2015). Though, excessive ROS generation by mitochondria will trigger mitophagy as a cell defense mechanism (Filomeni et al., 2015). Earlier study corroborates the specificity of ROS generation by NADH dehydrogenase mitochondrial complex (Galam et al., 2015) thus the observed complex I inhibitory effect by 4-HNE suggests possible myotube hormesis in response to stress. Indeed, here we show that the myotubes demonstrated transient adaptation to the acute stress with physiological 4-HNE concentrations but not in the case with higher concentration. The

4-HNE induced hormesis was further supported by upregulation of 11 mitochondrial metabolism genes 24 hours after exposure. Impressive effect of 4-HNE on the big number of mitochondrial genes advocated mitochondrial biogenesis. Indeed, a dose dependent increase in mitochondrial density was noticed 24 hours after acute exposure to 4-HNE. It is possible that 4-HNE could be one of the mechanisms that evokes mitochondrial biogenesis process as a physiological adaptation to endurance exercise (Hyatt et al., 2015).

In summary, our results make evident for the first time that pathological 4-HNE levels elicit damaging effects on skeletal muscle cells while acute exposure to physiological 4-HNE induces transient adaptation. Our ongoing research findings further signify the importance of skeletal muscle cells hormesis in response to acute stress in order to maintain essential biological functions.

Acknowledgements

Financial support and sponsorship: This study was supported by the Anti Doping Lab Qatar.

Author Contributions

Investigation, A.S.A., S.B., P.R.A., A.Y.A. and M.J.; Methodology, A.S.A., S.B., P.R.A., A.Y.A. and M.J.; Formal Analysis, A.S.A., P.R.A., A.B., P.H., A.Y.A. and M.J.; Writing – Original Draft, A.S.A., P.R.A., A.B., P.H., A.Y.A. and M.J.; Writing – Review & Editing, A.Y.A. and M.J.; Supervision, A.Y.A. and M.J.

Declaration of Interests

The authors declare no competing interests.

Figure Legends

Figure 1. Low dose caffeine stimulates sustained $[Ca^{2+}]_c$ oscillations in rat skeletal myotubes. Short (A) or prolonged exposure of rat myocytes to 1 mM caffeine induced sustained $[Ca^{2+}]_c$ oscillations that continued for hours. At 5 mM, caffeine (B) stimulated an initial $[Ca^{2+}]_c$ spike followed by faster oscillations, while at 10 mM (C) it caused a large $[Ca^{2+}]_c$ spike followed by a sustained elevation. This signal was prevented by ryanodine receptor inhibitor, 20μM dantrolene (D).

Figure 2. Caffeine activated ROS production induce lipid peroxidation in myotubes. The effect with caffeine on myotubes cellular redox homeostasis and peroxidation of lipids. A. Effect of 2-hour incubation of C2C12 myotubes with various concentrations of caffeine on cell viability, B. Impact of caffeine and on superoxide production measured by DHE fluorescence (Ex 530 nm / Em 580 nm) over 40 min, 20 μM dentrolene was preicubated for 20 min before adding of 10 mM caffeine C. The rate of DHE fluorescence under application of caffeine expressed as mean values (±SD) between 10 to 30 min in % of control. D. & E. Peroxidation of lipids analyzed by BODIPY581/591 C11 [495/521nm (oxidized) and 575/600nm (non-oxidized)]. F. Caffeine induced 4-HNE adduct formation. Mean values (±SD) are given: (*) significance $P<0.05$ in comparison to control untreated myotubes; (**) $P<0.001$.

Figure 3. Product of lipid peroxidation activates non pathological production of ROS. The effect of 24-hour exposure to 4-HNE on C2C12 myotubes viability and cellular redox homeostasis. A. The effect of 24-hour exposure to 4-HNE on myotubes viability. B. 4-HNE induced dose dependent effect on myotubes morphology and viability. C. The effect of different 4-HNE concentrations on intracellular ROS production measured by DCFH-DA assay (Ex 500 nm / Em 529 nm) and D. superoxide production measured by DHE fluorescence (Ex 530 nm / Em 580 nm). Mean values (±SD) for 5-replicates of representative experiment is given: (*) significance $P<0.05$ in comparison to control untreated myotubes.

Figure 4. The immediate effect of 4-HNE on mitochondrial function. A. Effect of 4-HNE on mitochondrial NADH autofluorescence of myotubes, scaled between a fully oxidised level induced by 1μM FCCP and the fully reduced state at 100% in response to 1mM NaCN. B. The bioenergetics profile of myotubes in response to 4-HNE (O – Oligomycin A, FCCP, R/A – Rotenone/Antimycin A injection). C. Quantitative data of maximal respiration, spare respiratory capacity and ATP production. Mean values

(±SEM) for 5-replicates of representative experiment is given: (*) significance P<0.05 in comparison to control untreated myotubes.

Figure 5. Hormetic effects of acute 4-HNE exposure on mitochondria. A. The bioenergetics profile of myotubes in response to 4-HNE (O – Oligomycin A, FCCP, R/A – Rotenone/Antimycin A injection). B. Quantitative data of basal respiration, maximal respiration, spare respiratory capacity and ATP production. Mean values (±SEM) for 5-replicates of representative experiment is given: (*) significance P<0.05 in comparison to control untreated myotubes. C. Effect of acute exposure to 10 μM 4-HNE on superoxide production. Mean values (±SEM) for 5-replicates of representative experiment is given: (*) significance P<0.05 in comparison to control untreated myotubes. D. Volcano plot displaying differentially expressed genes between control and 4-HNE treated myotubes. The y-axis is the mean expression value of negative log 10 (p-value), and the x-axis is the log2 fold change value. The colored dots represent the up regulated expressed transcripts ($p < 0.05$) of myotubes treated with 2.5 μM (triangle), 5 μM (square) or 10 μM (circle). Colors represent different complexes: Complex I (red), Complex II (green), Complex III (blue) and Complex V (yellow). E. & F. The effect of overnight treatment of 4-HNE on mitochondrial density measured using MitoTracker (Images were taken at 20X). G. Heat map of mitochondrial metabolism genes.

References

Andringa, K.K., Udoh, U.S., Landar, A., and Bailey, S.M. (2014). Proteomic analysis of 4-hydroxynonenal (4-HNE) modified proteins in liver mitochondria from chronic ethanol-fed rats. Redox Biol *2C*, 1038-1047.

Angelova, P.R., and Abramov, A.Y. (2016). Functional role of mitochondrial reactive oxygen species in physiology. Free Radic Biol Med *100*, 81-85.

Bartolome, F., Esteras, N., Martin-Requero, A., Boutoleau-Bretonniere, C., Vercelletto, M., Gabelle, A., Le Ber, I., Honda, T., Dinkova-Kostova, A.T., Hardy, J., Carro, E., Abramov, A.Y. (2017) Pathogenic p62/SQSTM1 mutations impair energy metabolism through limitation of mitochondrial substrates. Sci Rep *7(1)*:1666.

Biasi, F., Vizio, B., Mascia, C., Gaia, E., Zarkovic, N., Chiarpotto, E., Leonarduzzi, G., and Poli, G. (2006). c-Jun N-terminal kinase upregulation as a key event in the proapoptotic interaction between transforming growth factor-beta1 and 4-hydroxynonenal in colon mucosa. Free Radic Biol Med *41*(3), 443-54.

Chapple, S.J., Cheng, X., and Mann, G.E. (2013). Effects of 4-hydroxynonenal on vascular endothelial and smooth muscle cell redox signaling and function in health and disease. Redox Biol *1*, 319-31.

Cheng, A.J., Yamada, T., Rassier, D.E., Andersson, D.C., Westerblad, H., and Lanner, J.T. (2016). Reactive oxygen/nitrogen species and contractile function in skeletal muscle during fatigue and recovery. J Physiol *594*(18), 5149-60.

Ding, S., Riddoch-Contreras, J., Abramov, A.Y., Qi, Z., and Duchen, M.R. (2012). Mild stress of caffeine increased mtDNA content in skeletal muscle cells: the interplay between Ca2+ transients and nitric oxide. J Muscle Res Cell Motil *33*(5), 327-37.

Domijan, A.M., and Abramov, A.Y. (2011). Fumonisin B1 inhibits mitochondrial respiration and deregulates calcium homeostasis--implication to mechanism of cell toxicity. Int J Biochem Cell Biol *43*(6), 897-904.

Domijan, A.M., Kovac, S., and Abramov, A.Y. (2014). Lipid peroxidation is essential for phospholipase C activity and the inositol-trisphosphate-related Ca^{2+} signal. J Cell Sci *127*(Pt 1), 21-6.

Duchen, M.R. (1999). Contributions of mitochondria to animal physiology: from homeostatic sensor to calcium signalling and cell death. J Physiol. *516* (Pt 1), 1-17.

Elrayess, M.A., Almuraikhy, S., Kafienah, W., Al-Menhali, A., Al-Khelaifi, F., Bashah, M., Zarkovic, K., Zarkovic, N., Waeg, G., Alsayrafi, M., and Jaganjac,

M. (2017). 4-hydroxynonenal causes impairment of human subcutaneous adipogenesis and induction of adipocyte insulin resistance. Free Radic Biol Med *104*, 129-137.

Esterbauer, H., Schaur, R.J., and Zollner, H. (1991). Chemistry and biochemistry of 4-hydroxynonenal, malonaldehyde and related aldehydes. Free Radic Biol Med *11*(1), 81-128.

Filomeni, G., De Zio, D., and Cecconi, F. (2015). Oxidative stress and autophagy: the clash between damage and metabolic needs. Cell Death Differ *22*(3), 377-88.

Galam, L., Failla, A., Soundararajan, R., Lockey, R.F., and Kolliputi, N. (2015). 4-hydroxynonenal regulates mitochondrial function in human small airway epithelial cells. Oncotarget *6*(39), 41508-21.

Gomez-Cabrera, M.C., Domenech, E., Romagnoli, M., Arduini, A., Borras, C., Pallardo, F.V., Sastre, J., and Viña, J. (2008). Oral administration of vitamin C decreases muscle mitochondrial biogenesis and hampers training-induced adaptations in endurance performance. Am J Clin Nutr *87*(1), 142-9.

Gong, M.C., Arbogast, S., Guo, Z., Mathenia, J., Su, W., and Reid, M.B. (2006). Calcium-independent phospholipase A2 modulates cytosolic oxidant activity and contractile function in murine skeletal muscle cells. J Appl Physiol (1985) *100*(2), 399-405.

Grumati, P., and Bonaldo, P. (2012). Autophagy in skeletal muscle homeostasis and in muscular dystrophies. Cells *1*(3), 325-45.

Hidalgo, C., Sánchez, G., Barrientos, G., and Aracena-Parks, P. (2006). A transverse tubule NADPH oxidase activity stimulates calcium release from isolated triads via ryanodine receptor type 1 S -glutathionylation. J Biol Chem *281*(36), 26473-82.

Huang, J.H., and Hood, D.A. (2009). Age-associated mitochondrial dysfunction in skeletal muscle: Contributing factors and suggestions for long-term interventions. IUBMB Life *61*(3), 201-14.

Hyatt, H.W., Toedebusch, R.G., Ruegsegger, G., Mobley, C.B., Fox, C.D., McGinnis, G.R., Quindry, J.C., Booth, F.W., Roberts, M.D., and Kavazis, A.N. (2015). Comparative adaptations in oxidative and glycolytic muscle fibers in a low voluntary wheel running rat model performing three levels of physical activity. Physiol Rep *3*(11) pii, e12619

Jaganjac, M., Cacev, T., Cipak, A., Kapitanovic, S., Gall Troselj, K., and Zarkovic, N. (2012). Even stressed cells are individuals: second messengers of free radicals in pathophysiology of cancer. Croat Med J *53*(4):304-9.

Jaganjac, M., Cipak, A., Schaur, R.J., and Zarkovic, N. (2016). Pathophysiology of neutrophil-mediated extracellular redox reactions. Front Biosci (Landmark Ed) *21*, 839-55.

Jaganjac, M., Matijevic, T., Cindric, M., Cipak, A., Mrakovcic, L., Gubisch, W., and Zarkovic, N. (2010). Induction of CMV-1 promoter by 4-hydroxy-2-nonenal in human embryonic kidney cells. Acta Biochim Pol *57*(2), 179-83.

Jaganjac, M., Tirosh, O., Cohen, G., Sasson, S., and Zarkovic, N. (2013). Reactive aldehydes--second messengers of free radicals in diabetes mellitus. Free Radic Res *47*, 39-48.

Kim, J.A., Wei, Y., and Sowers, J.R. (2008). Role of mitochondrial dysfunction in insulin resistance. Circ Res *102*(4), 401-14.

Lantier, L., Fentz, J., Mounier, R., Leclerc, J., Treebak, J.T., Pehmøller, C., Sanz, N., Sakakibara, I., Saint-Amand, E., Rimbaud, S., et al. (2014). AMPK controls exercise endurance, mitochondrial oxidative capacity, and skeletal muscle integrity. FASEB J. *28*(7), 3211-24. doi: 10.1096/fj.14-250449..

Leonarduzzi, G., Robbesyn, F., and Poli, G. (2004). Signaling kinases modulated by 4-hydroxynonenal. Free Radic Biol Med *37*, 1694-702.

McArdle, A., Pattwell, D., Vasilaki, A., Griffiths, R.D., and Jackson, M.J. (2001). Contractile activity-induced oxidative stress: cellular origin and adaptive responses. Am J Physiol Cell Physiol *280*(3), C621-7.

Parker, N., Vidal-Puig, A., and Brand, M.D. (2008). Stimulation of mitochondrial proton conductance by hydroxynonenal requires a high membrane potential. Biosci Rep *28*(2), 83-8.

Pattwell, D.M., McArdle, A., Morgan, J.E., Patridge, T.A., and Jackson, M.J. (2004). Release of reactive oxygen and nitrogen species from contracting skeletal muscle cells. Free Radic Biol Med *37*(7), 1064-72.

Poljak-Blazi, M., Jaganjac, M., Sabol, I., Mihaljevic, B., Matovina, M., and Grce, M. (2011). Effect of ferric ions on reactive oxygen species formation, cervical cancer cell lines growth and E6/E7 oncogene expression. Toxicol In Vitro *25*(1), 160-6.

Schaur, R.J., Siems, W., Bresgen, N., and Eckl, P.M. (2015). 4-Hydroxy-nonenal-A Bioactive Lipid Peroxidation Product. Biomolecules *5*(4), 2247-337.

Steinbacher, P., and Eckl, P. (2015). Impact of oxidative stress on exercising skeletal muscle. Biomolecules *5*(2), 356-77.

Uchida, K. (2003). 4-Hydroxy-2-nonenal: a product and mediator of oxidative stress. Prog Lipid Res *42*, 318-43.

Vaarmann, A., Gandhi, S., and Abramov, A.Y. (2010). Dopamine induces Ca2+ signaling in astrocytes through reactive oxygen species generated by monoamine oxidase. J Biol Chem *285*(32), 25018-23.

Yang, Y., Sharma, R., Sharma, A., Awasthi, S., and Awasthi, Y.C. (2003). Lipid peroxidation and cell cycle signaling: 4-hydroxynonenal, a key molecule in stress mediated signaling. Acta Biochim Pol *50*(2), 319-36.

Zarkovic, N. (2003). 4-hydroxynonenal as a bioactive marker of pathophysiological processes. Mol Aspects Med. *24*, 281-91.

Zarkovic, N., Cipak, A., Jaganjac, M., Borovic, S., and Zarkovic, K. (2013). Pathophysiological relevance of aldehydic protein modifications. J Proteomics *92*, 239-47.

Zhao, Y., Miriyala, S., Miao, L., Mitov, M., Schnell, D., Dhar, S.K., Cai, J., Klein, J.B., Sultana, R., Butterfield, D.A., et al. (2014). Redox proteomic identification of HNE-bound mitochondrial proteins in cardiac tissues reveals a systemic effect on energy metabolism after doxorubicin treatment. Free Radic Biol Med *72*, 55-65.

Zivkovic, M., Zarkovic, K., Skrinjar, Lj., Waeg, G., Poljak-Blazi, M., Borovic, S., Schaur, R.J., and Zarkovic, N. (2005) A new method for detection of HNE-histidine conjugates in rat inflammatory cells. Croatica Chemica Acta *78*, 91-98.

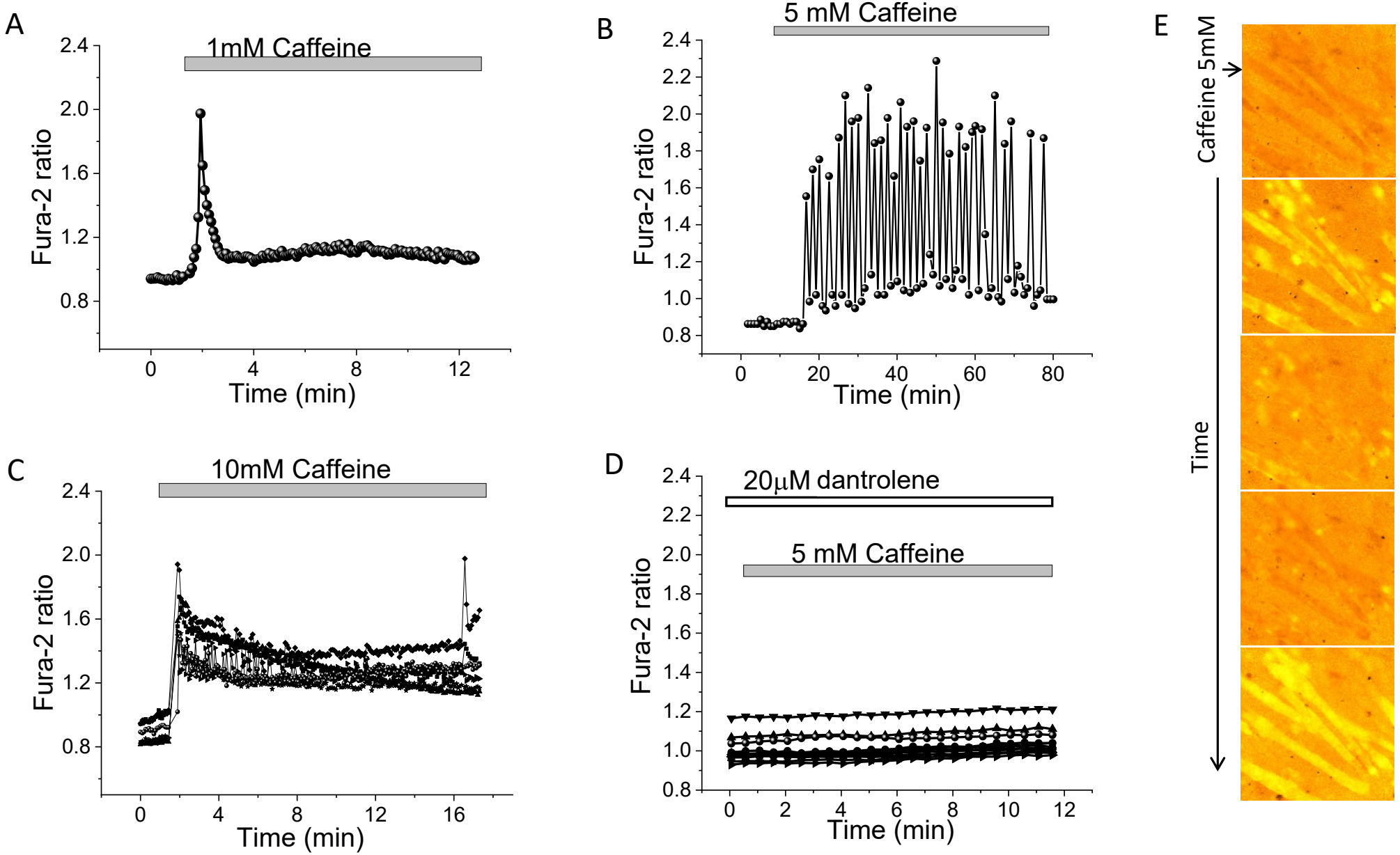
A
1mM Caffeine
Fura-2 ratio
Time (min)
B
5 mM Caffeine
Fura-2 ratio
Time (min)
C
10mM Caffeine
Fura-2 ratio
Time (min)
D
20μM dantrolene
5 mM Caffeine
Fura-2 ratio
Time (min)
E
Caffeine 5mM
Time

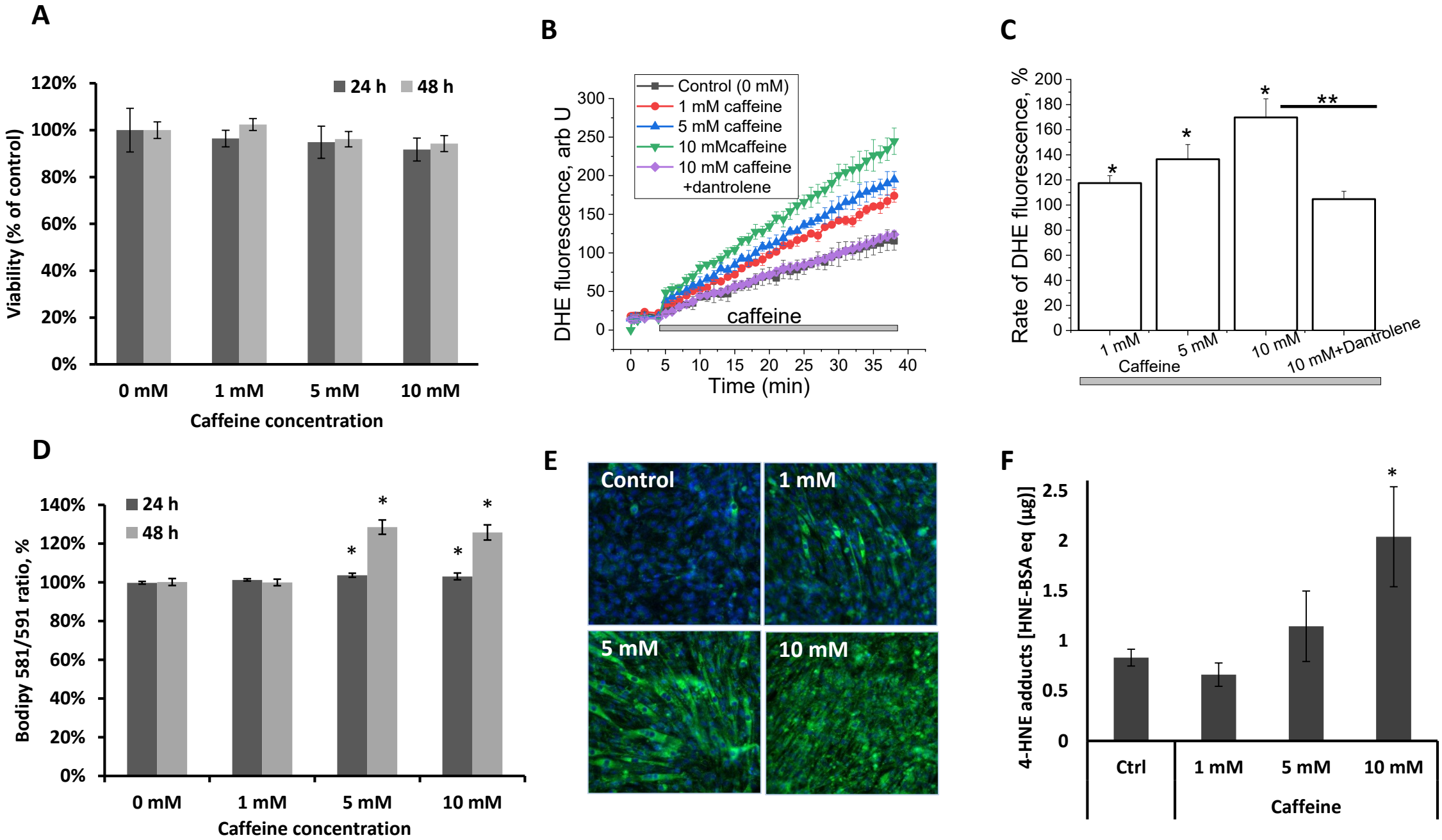
A
120%
100%
80%
60%
40%
20%
0%
Viability (% of control)
24 h
48 h
0 mM
1 mM
5 mM
10 mM
Caffeine concentration
B
Control (0 mM)
1 mM caffeine
5 mM caffeine
10 mMcaffeine
10 mM caffeine
+dantrolene
DHE fluorescence, arb U
300
250
200
150
100
50
0
caffeine
0
5
10
15
20
25
30
35
40
Time (min)
C
Rate of DHE fluorescence, %
200
180
160
140
120
100
80
60
40
20
0
*
*
*
**
1 mM
5 mM
10 mM
10 mM+Dantrolene
Caffeine
D
140%
120%
100%
80%
60%
40%
20%
0%
Bodipy 581/591 ratio, %
24 h
48 h
*
*
*
*
0 mM
1 mM
5 mM
10 mM
Caffeine concentration
E
Control
1 mM
5 mM
10 mM
F
4-HNE adducts [HNE-BSA eq (µg)]
2.5
2
1.5
1
0.5
0
*
Ctrl
1 mM
5 mM
10 mM
Caffeine

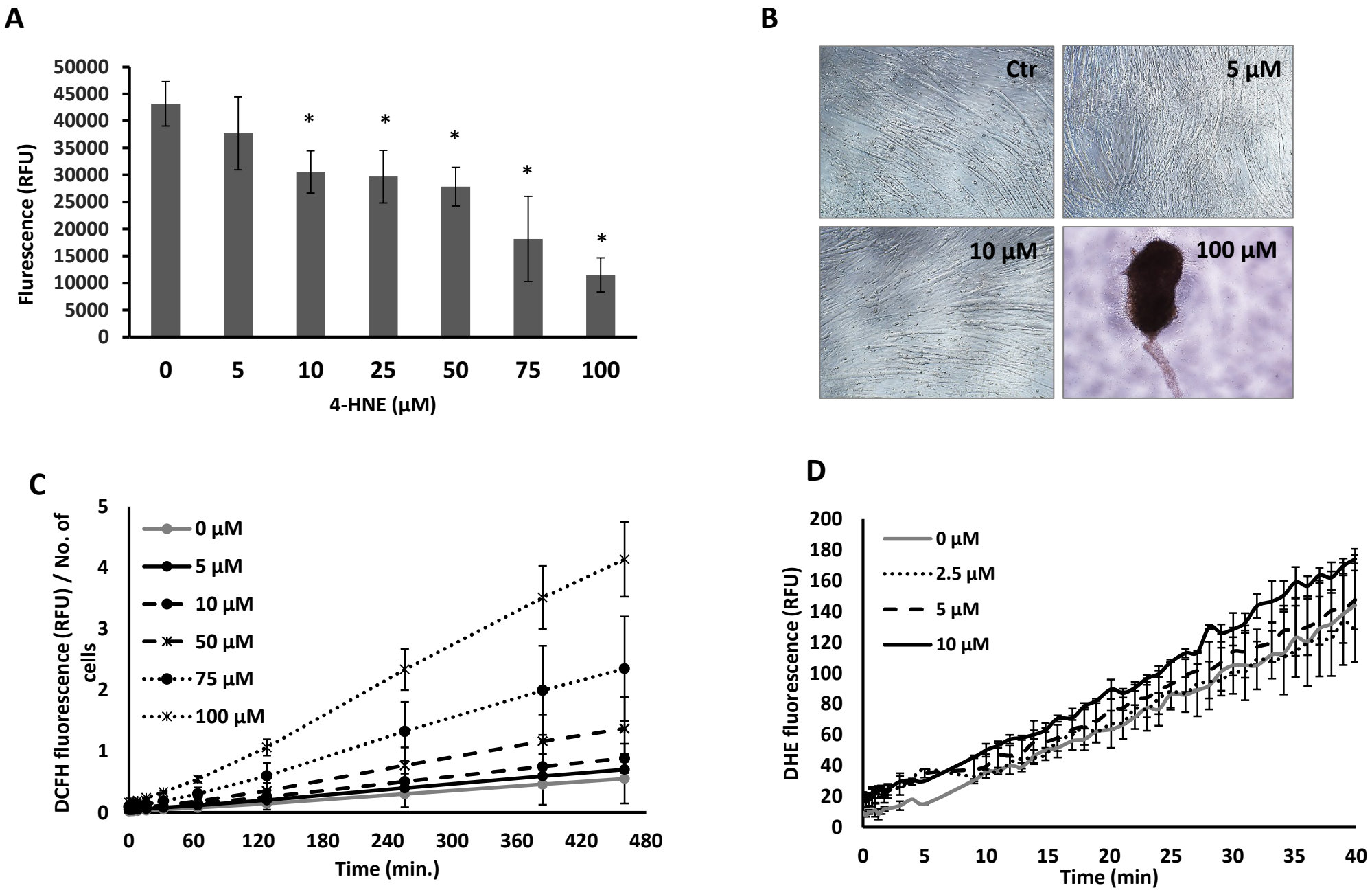
A
Flurescence (RFU)
50000
45000
40000
35000
30000
25000
20000
15000
10000
5000
0
0
5
10
25
50
75
100
4-HNE (μM)
B
Ctr
5 μM
10 μM
100 μM
C
DCFH fluorescence (RFU) / No. of cells
0 μM
5 μM
10 μM
50 μM
75 μM
100 μM
Time (min.)
D
DHE fluorescence (RFU)
0 μM
2.5 μM
5 μM
10 μM
Time (min)

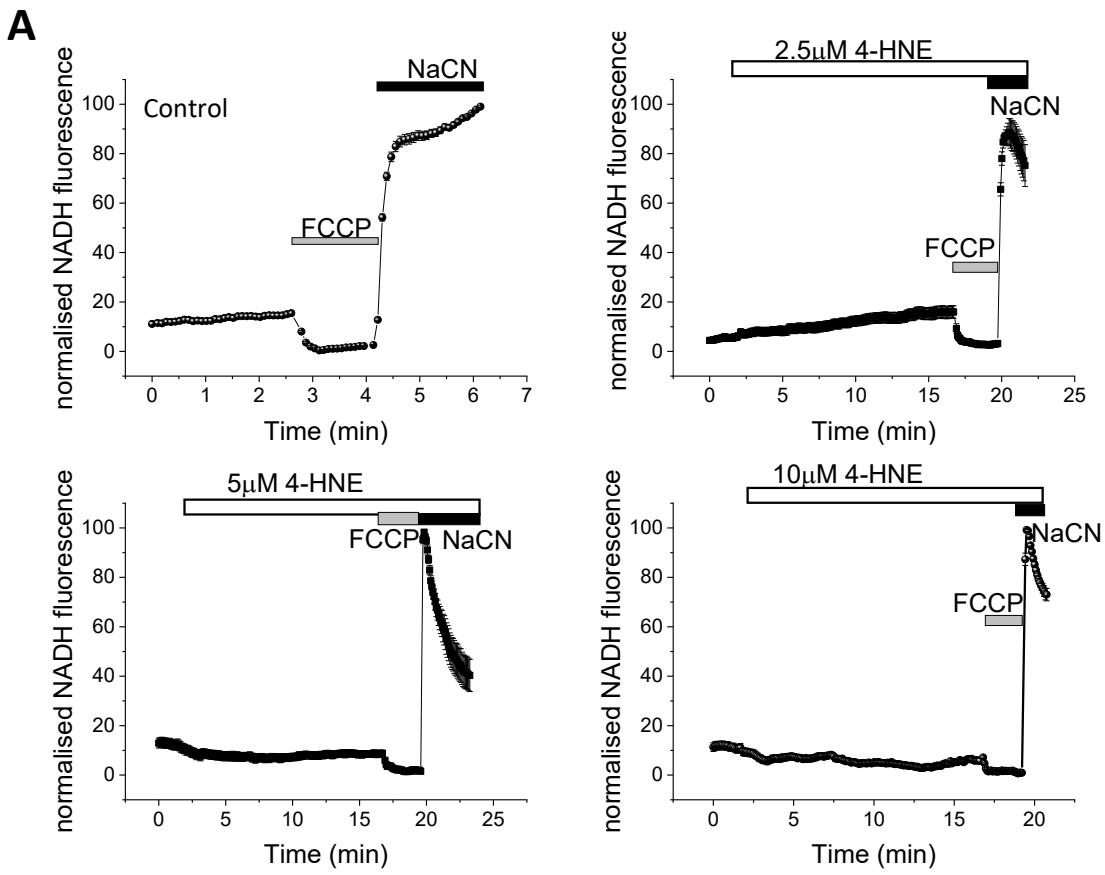
A
Control
NaCN
FCCP
2.5μM 4-HNE
5μM 4-HNE
10μM 4-HNE
normalised NADH fluorescence
Time (min)

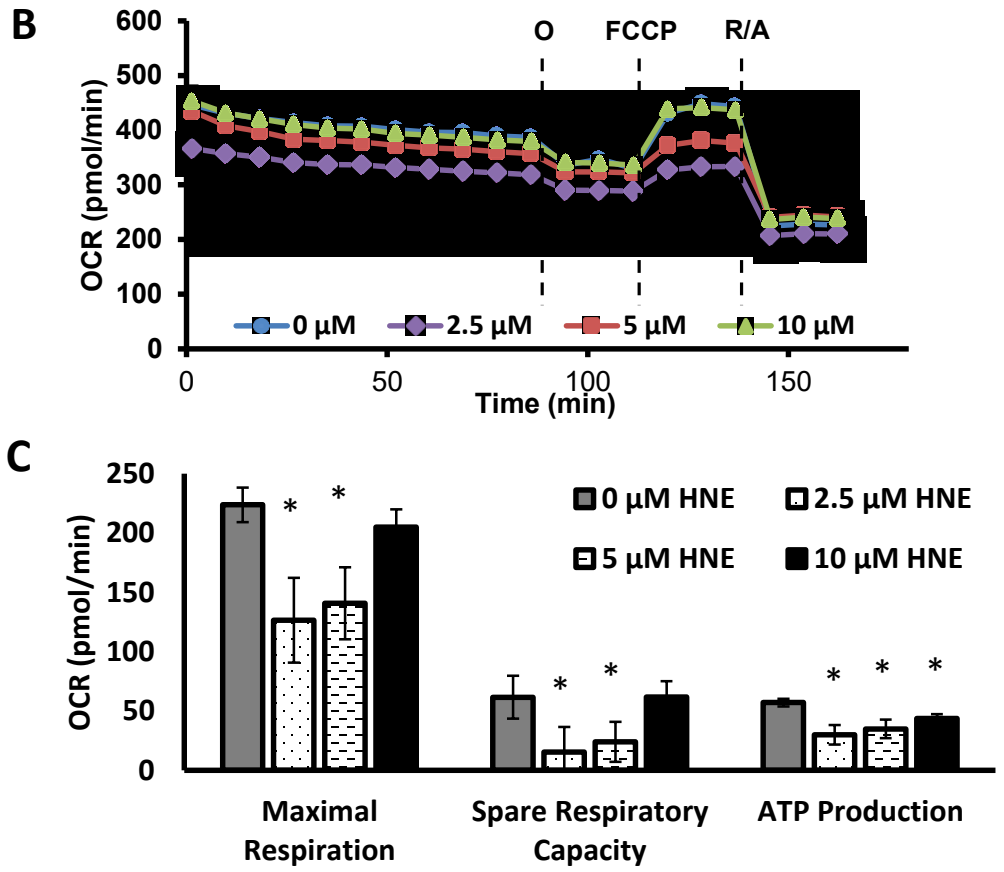
B
C
O
FCCP
R/A
OCR (pmol/min)
Time (min)
0 μM
2.5 μM
5 μM
10 μM
0 μM HNE
2.5 μM HNE
5 μM HNE
10 μM HNE
Maximal Respiration
Spare Respiratory Capacity
ATP Production

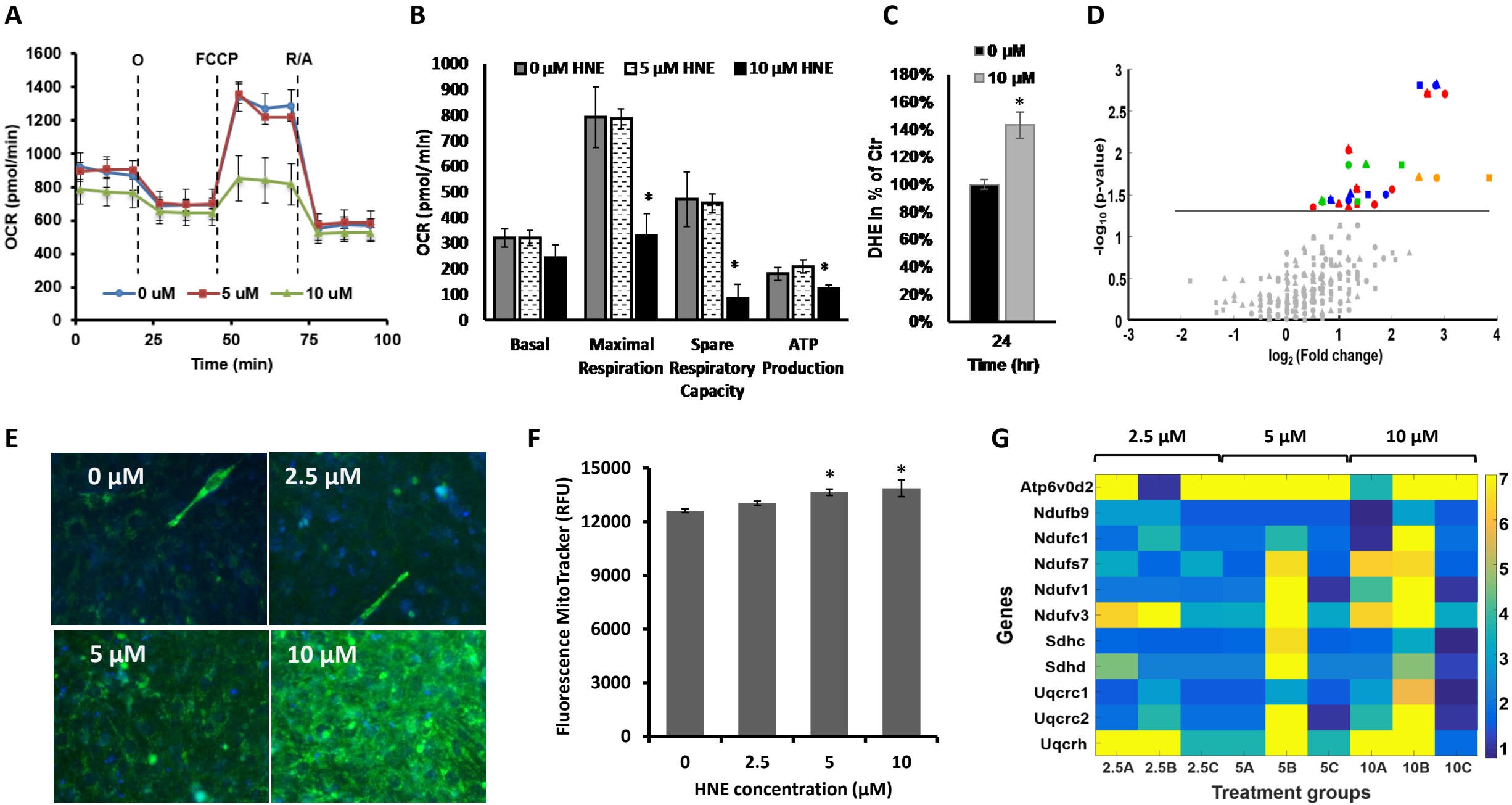
A
O
FCCP
R/A
OCR (pmol/min)
Time (min)
0 uM
5 uM
10 uM
B
0 µM HNE
5 µM HNE
10 µM HNE
OCR (pmol/min)
Basal
Maximal Respiration
Spare Respiratory Capacity
ATP Production
C
0 µM
10 µM
DHE In % of Ctr
24
Time (hr)
D
-log10 (p-value)
log2 (Fold change)
E
0 µM
2.5 µM
5 µM
10 µM
F
Fluorescence MitoTracker (RFU)
HNE concentration (µM)
G
2.5 µM
5 µM
10 µM
Genes
Atp6v0d2
Ndufb9
Ndufc1
Ndufs7
Ndufv1
Ndufv3
Sdhc
Sdhd
Uqcrc1
Uqcrc2
Uqcrh
2.5A
2.5B
2.5C
5A
5B
5C
10A
10B
10C
Treatment groups